Quaternary Science Reviews 324 (2024) 108465

Contents lists available at ScienceDirect

Quaternary Science Reviews

journal homepage: www.elsevier.com/locate/quascirev

Contrasting north-south pattern in Holocene lacustrine carbon accumulation in China: Summer monsoon dynamics and human disturbance

Hanxiang Liu [b], Mengdi Jiang [a,g,**], Zicheng Yu [d,e], Wengang Kang [a], Zhongwei Shen [f], Haoran Dong [c], Shengqian Chen [a], Xinwei Yan [c], Jianbao Liu [a,c,*]

[a] *Group of Alpine Paleoecology and Human Adaptation (ALPHA), State Key Laboratory of Tibetan Plateau Earth System, Environment and Resources (TPESER), Institute of Tibetan Plateau Research, Chinese Academy of Sciences, Beijing, 100101, China*
[b] *College of Geography and Environmental Sciences, Zhejiang Normal University, Jinhua, 321004, China*
[c] *Key Laboratory of Western China's Environmental Systems (Ministry of Education), College of Earth and Environmental Science, Center for Pan Third Pole Environment (Pan-TPE), Lanzhou University, Lanzhou, 730000, China*
[d] *Key Laboratory of Geographical Processes and Ecological Security in Changbai Mountains (Ministry of Education), School of Geographical Sciences, Northeast Normal University, Changchun, 130024, China*
[e] *State Key Laboratory of Black Soil Conservation and Utilization, Northeast Institute of Geography and Agroecology, Chinese Academy of Sciences, Changchun, 130102, China*
[f] *School of Geographic Sciences, Hunan Normal University, Changsha, 410081, China*
[g] *University of Chinese Academy of Sciences, Beijing, 100049, China*

ARTICLE INFO

Handling Editor: Dr P Rioual

Keywords:
Carbon accumulation rate
Lake-catchment ecosystem
Precipitation
Vegetation cover
Human activities
Erosion

ABSTRACT

Some studies suggest that the lacustrine carbon (C) accumulation has gradually increased during the Holocene in the monsoon region of eastern China, primarily due to the intensified human land use. However, other studies argue that the highest C accumulation in China's lakes occurred in the early Holocene, influenced by high summer insolation. The pattern and driving forces behind Holocene lacustrine C accumulation in eastern China remain controversial. In this study, carbon accumulation rate (CAR) records from eleven lakes in northern China and eight lakes in southern China were synthesized to examine variations in CAR between the two regions and to understand the factors driving these variations. The results reveal that CAR in northern China increased between 11 and 6 thousand calendar years before present (cal ka BP), as the strengthening summer monsoon resulted in increased precipitation, promoting the growth of vegetation in the lake's catchments and subsequently increasing terrestrial sediment and C input into lakes. Conversely, CAR in southern China decreased due to reduced precipitation, leading to a decline in sedimentation rate and C inputs in the lakes. After 6 cal ka BP, decreased precipitation and increased human activities in northern China reduced the forest cover, resulting in a decline in C input into lakes without reducing sediment inputs, which consequently led to a decrease in CAR. In southern China, higher precipitation and intensified human activities significantly increased sediment inputs without affecting C inputs, resulting in an increasing trend in CAR. Thus, human activities and the dipole pattern of precipitation created an inverse phase of C accumulation between northern and southern China in lakes throughout the Holocene. The study also highlights the importance of terrestrial C from the catchment in contributing to lacustrine C accumulation on large regional scale, as C in lake sediments was found to be closely associated with forest cover in the catchment.

* Corresponding author. Group of Alpine Paleoecology and Human Adaptation (ALPHA), State Key Laboratory of Tibetan Plateau Earth System, Environment and Resources (TPESER), Institute of Tibetan Plateau Research, Chinese Academy of Sciences, Beijing 100101, China.
** Corresponding author. Group of Alpine Paleoecology and Human Adaptation (ALPHA), State Key Laboratory of Tibetan Plateau Earth System, Environment and Resources (TPESER), Institute of Tibetan Plateau Research, Chinese Academy of Sciences, Beijing, 100101, China.
E-mail addresses: mdjiang@itpcas.ac.cn (M. Jiang), jbliu@itpcas.ac.cn (J. Liu).

https://doi.org/10.1016/j.quascirev.2023.108465
Received 11 September 2023; Received in revised form 4 December 2023; Accepted 5 December 2023

1. Introduction

The carbon (C) cycle plays a crucial role in regulating Earth's climate, and lakes sediments are a significant, long-term sink for C at regional to global scales during the Holocene (Armstrong, 2010; Kortelainen et al., 2004). Understanding the fate of C buried by lakes under future climate change and human activities requires identifying the influencing factors of C accumulation dynamics. Currently, there are few studies on C accumulation in Chinese lakes during the Holocene, while a debate on the changing trends and driving factors of C accumulation is ongoing. Wang et al. (2015) considered that the sediment and C accumulation of lakes in eastern China had an overall rising trend since 12 cal ka BP based on the synthesis of lake sediments records, corresponding to terrestrial organic matter input due to land-use change. However, some studies suggest that most lakes in China had a higher rate of C burial during the Holocene thermal maximum in the early and middle Holocene than in the modern period. This was likely due to larger influx of terrestrial organic matter and increased productivity in lakes under warm and humid climate conditions at that time (Hao et al., 2021; Zhang et al., 2013). The factors influencing carbon accumulation in lakes include lake size (Dong et al., 2012), climate change (Gudasz et al., 2010), and human activities (Anderson et al., 2020; Chen et al., 2015c). Given the complex and diverse nature of these factors in different lakes, the spatial and temporal patterns of lake carbon accumulation rates and their driving factors on a millennium scale in China during the Holocene period remain unclear.

Precipitation, temperature, and human activities are common factors that affect C accumulation in most lakes across China. Through sediment records and instrumental data, it has been observed that northern and southern China experience a dipole pattern of precipitation (Chen et al., 2015b; Ding et al., 2008; Liu et al., 2020). This pattern is influenced by the movement of the Western Pacific Subtropical High (WPSH), which enables the rainfall belt to move north or south of China under the control of the East Asian Summer Monsoon (EASM). The varying precipitation levels directly impact the growth of arboreal vegetation and contribute to soil erosion within the catchment. The temperature factor plays a significant role in lacustrine C accumulation by influencing the growth and decay of both terrestrial and aquatic vegetation. Remarkably, the temperature patterns in northern and southern China during the Holocene period were found to be similar (Ge et al., 2013). This can be attributed to a relatively consistent driving mechanism for millennium-scale temperature changes (Kaufman et al., 2020; Liu et al., 2014). In addition, both northern and southern China have a long history of intense human activities, particularly land use practices (Cohen, 2011). Deforestation, farmland reclamation, and other human-induced changes significantly impact the amount of C entering lakes. These activities alter the carbon dynamics within the lake's catchment, ultimately influencing C accumulation. To summarize, the difference in lacustrine carbon accumulation between northern and southern China is mainly driven by difference in precipitation. Comparing the synthetic lacustrine carbon data from both regions can yield valuable insights into the various variables that affect carbon accumulation in lakes.

This study selected eleven lakes in northern China and eight lakes in southern China, following specific criteria, to examine their carbon accumulation rate (CAR) records. The reliable reconstruction data for paleo-precipitation and paleo-vegetation in both regions were compared with the synthesized CAR records. The study aims to determine the lacustrine C dynamics and its controlling factors on a large regional scale in northern and southern China during the Holocene, and resolve the dispute over the change in Holocene C accumulation and driving mechanism of lakes in the monsoon region of eastern China from the perspective of distinguishing between northern and southern lakes. The findings of this study also offer fundamental knowledge for predicting lacustrine C change under future climate scenarios.

2. Materials and methods

2.1. Study region

China's natural division into northern and southern regions is demarcated by the Qin-Huai line, which follows the Qinling Mountains and the Huai River at approximately 33°N latitude. The Qin-Huai line aligns with the 0 °C isotherm in January and the 800-mm isohyet, distinguishing the vegetation types between the two regions. Northern China predominantly features a temperate mix of broadleaf-conifer and broadleaved deciduous forests, while southern China is characterized by subtropical evergreen broadleaved forests.

In northern China, summers are hot and rainy, while winters are cold and dry. As a result, vegetation growth and carbon input into lakes predominantly occur during the summer season. On the other hand, southern China experiences hot and rainy summers, alongside mild and less rainy winters. This allows for year-round vegetation growth, providing continuous carbon sources for lakes.

2.2. Criteria for selecting sediment records

Numerous lake sediment records from both northern and southern China have been published. To achieve the objectives of this research, three criteria were used to select suitable sediment records. The first criterion necessitated that the record span most of the Holocene period without significant sedimentary gaps. The second criterion required the availability of independently determined ages for the sediment records, with a sufficient time resolution to determine their occurrence in the early, middle, or late Holocene (at least one date per 3000 years on average). The third criterion mandated the inclusion of data on total organic carbon (TOC) content in the records. Following these criteria, a total of ten lakes from northern China and seven lakes from southern China were chosen from the existing literature. Detailed information about the sites can be found in Fig. 1 and Table 1.

2.3. Statistical analyses

We compiled multiple ^{14}C ages from available published sources across northern and southern China (Table S1). We reconstructed a Bayesian depth-age chronology with Bacon for each lake core using the compiled ^{14}C ages. The sediment accumulation rate (SR, cm yr^{-1}) was calculated based on the chronology of the lake sediments according to the following formula:

$$SR = \frac{h}{t} \tag{1}$$

where h (cm) is the thickness of the sediment during time t (yr).

For records without dry bulk density (*DBD*, g cm^{-3}) data, *DBD* values were estimated using the following two equations (Kastowski et al., 2011):

$$DBD = 1.665 \times (TOC)^{-0.887} \tag{2}$$

when $TOC > 6\%$;

$$DBD = 1.776 - 0.363 \times \ln(10 \times TOC) \tag{3}$$

when $TOC \leq 6\%$.

Based on the chronologies, *TOC* (%), and the estimated *DBD* (g cm^{-3}), the apparent *CAR* (g C $m^{-2}yr^{-1}$) was calculated using the following:

$$CAR = SR \times DBD \times TOC \times 100 \tag{4}$$

All *TOC*, *SR*, and *CAR* data of the sediments were resampled in 400-year bins and then standardized using this formula:

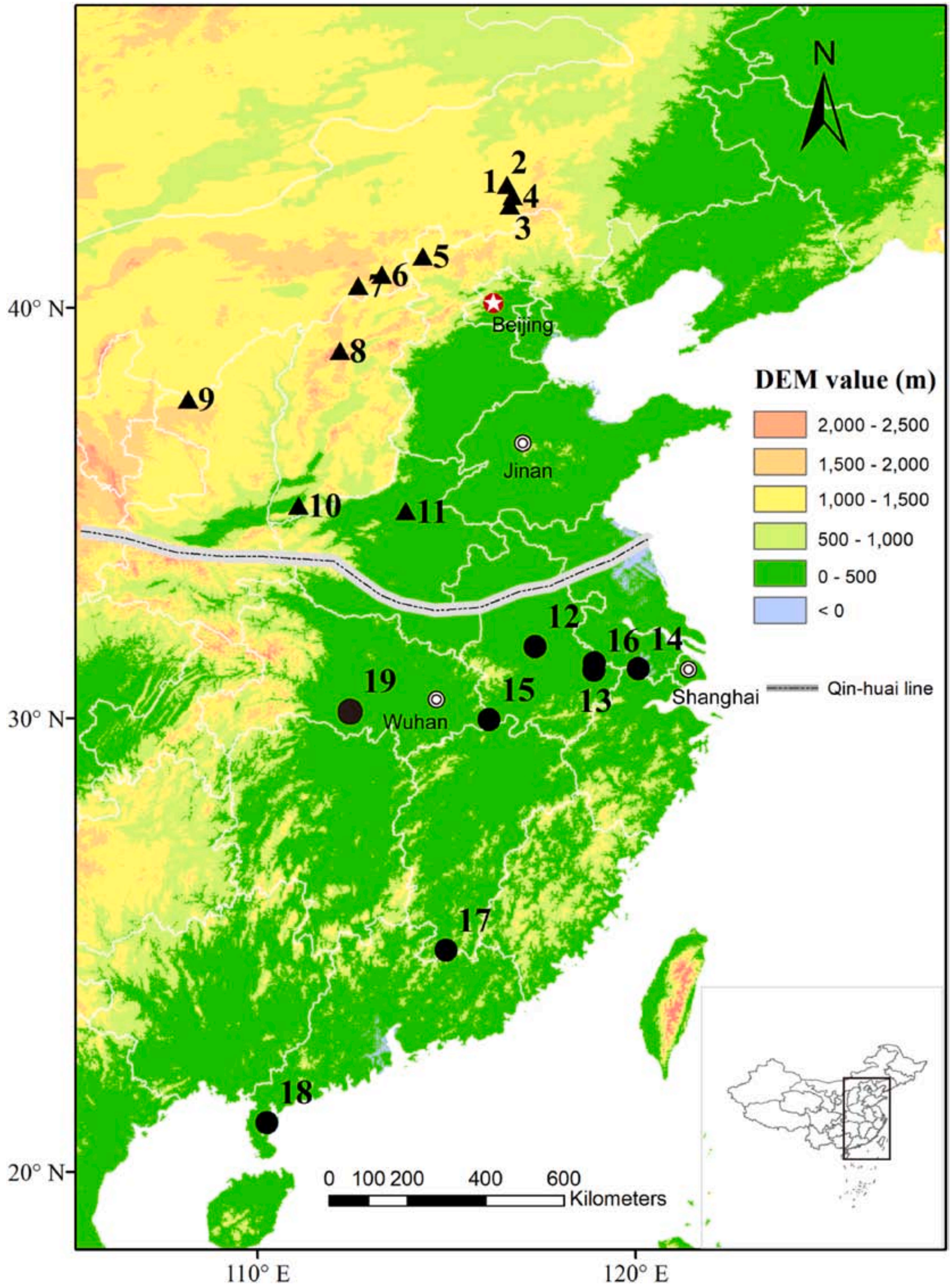

Fig. 1. Distribution of lake sites for carbon accumulation records (used in this study) in northern (triangles) and southern (circles) China. Inset show study region (rectangle) in China.

$$Zscore = \frac{X - \mu}{\sigma} \tag{5}$$

where *Z-score* is the standardized score; X is the raw value of *TOC*, *SR*, and *CAR*; μ is the mean value of all X; and σ is the standard deviation of X.

We used Generalized Additive Models (GAMs) regression—a type of regression model that uses smoothing splines instead of linear coefficients for covariates (Hastie and Tibshirani, 1986) to establish the relationship between CAR and influencing factors in northern and southern China.

2.4. Precipitation, pollen, and human activities records from northern and southern China

In order to investigate past changes in monsoon precipitation in northern and southern China, various archives and proxies have been utilized. In northern China, the synthesis of the paleosol record (Li et al., 2014) and pollen-based precipitation record (Li et al., 2018) has been employed to reflect the regional moisture. In southern China, the

Table 1
Site information on the sediment records used in carbon accumulation synthesis in lakes in this study.

Area	No.	Site name	Latitude (°N)	Longitude (°E)	Elevation (m a.s.l.)	Mean temporal resolution (yr)	References
North	1	Dali (DL)	43.2664	116.6066	1224	15	Xiao et al. (2008)
	2	Liuzhouwan (LZW)	42.7073	116.6830	1403	66	Wang et al. (2001)
	3	Haoluku1 (HLK1)	42.9563	116.7570	1343	48	Wang et al. (2001)
	4	Haoluku2 (HLK2)	42.9506	116.7936	1295	22	Liu et al. (2018)
	5	Angula (AGL)	41.3478	114.3777	1324	10	Wang et al. (2010)
	6	Huangqihai (HQH)	40.8250	113.2771	1262	10	Hao et al. (2014)
	7	Daihai (DHI)	40.5655	112.6644	1225	11	Xiao et al. (2006)
	8	Gonghai (GH)	38.9081	112.2342	1855	16	Chen et al. (2015a)
	9	Midiwan (MDW)	37.6500	108.6166	1349	13	Zhou et al. (1996)
	10	Yanhu (YH)	35.0341	111.0981	326	12	Li (2019)
	11	Zhengzhou PT (PT)	34.7450	113.8119	86	7	Wang et al. (2019)
South	12	Chaohu (CH)	31.6520	117.3782	4	13	Hu et al. (2015)
	13	Guchenghu (GCH)	31.2727	118.9213	5	8	Wang et al. (1996)
	14	Taihu (TH)	31.1175	120.1185	0	6	Ding (2004)
	15	Longganhu (LGH)	29.9374	116.1954	10	9	Yang et al. (2002)
	16	Nanyihu (NYH)	31.0833	118.9333	7	25	Dong et al. (2024)
	17	Dahu (DH)	24.7514	115.0339	269	56	Zhou et al. (2005)
	18	Huguangyan (HGY)	21.1500	110.2833	26	16	Yancheva et al. (2007)
	19	Jiangling (JL)	30.0418	112.4247	40	15	Wang et al. (2006)

hopanoid flux of the Dajiuhu peatland (Xie et al., 2013), the carbon preference index (CPI) values of n-alkanes in the Dahu Lake (Zhou et al., 2005), the isothermal remanent magnetization (IRM) record from Heshang Cave (Zhu et al., 2017), and the ratio of Rb/Sr in the sediments of Nanyihu Lake (Liu et al., 2020) have also been synthesized to assess regional moisture in this area.

The pollen data must include the ratio of arboreal plants to non-arboreal plants (AP/NAP), and must cover the entire duration of the Holocene. Based on this, we selected pollen records from Gonghai Lake (Chen et al., 2015a) and Daihai Lake (Xu et al., 2010) to verify each other in northern China. In addition, we also selected three pollen records from Nanyihu Lake (Chen et al., 2021), Dahu Lake (Zhou et al., 2004), and Huguangyan Lake (Wang et al., 2007) in southern China.

To assess the intensity of human activities, multiple indicators have been utilized in both northern and southern China. These include the density average estimates for the archaeological sites (Hosner et al., 2016), the proportion of domesticated rice in the lower Yangtze River region (Ma et al., 2018), and historical cropland area estimates in China (Goldewijk et al., 2017). These indicators help to provide insights into human influences on the environment in these regions.

3. Results

3.1. Variations of total organic C content

The TOC content in northern lakes ranged from 0.02% to 40% (Fig. S1), while in southern lakes, it varied between 0.04% and 20% (Fig. S2). The calculated DBD trends demonstrated an opposite pattern to TOC trends. Regarding the combined TOC Z-score of northern lakes (Fig. 3a and 5a), an increasing trend was observed from 11 to 6 cal ka BP, followed by a decreasing trend from 6 to 0 cal ka BP. Conversely, in southern lakes (Fig. 3b and 5f), the TOC Z-score decreased from 11 to 6 cal ka BP and remained stable between 6 and 0 cal ka BP.

3.2. Temporal and spatial patterns of sediment and C accumulation rates

The SR of the lake sediments in northern China ranged from 0.01 to 0.4 cm yr^{-1}, as shown in Fig. S3, while in southern China, it varied from 0.006 to 0.3 cm yr^{-1} (Fig. S4). Among the northern lakes, Liuzhouwan had the lowest average SR of 0.015 cm yr^{-1}, while Midiwan had the highest average SR of 0.2 cm yr^{-1}. In the case of southern lakes, Dahu had the lowest average SR of 0.015 cm yr^{-1}, while Taihu had the highest average SR of 0.15 cm yr^{-1}. The combined SR Z-score of northern lakes exhibited high values during the period of 3–2 cal ka BP and at 12 cal ka BP (Fig. 3c and 5b), whereas the combined SR Z-score of southern lakes displayed high values around 7 cal ka BP and showed an increasing trend from 6 to 0 cal ka BP (Fig. 3e and 5h).

Moving on to the CAR, most lakes in northern China had CAR values ranging from 0.05 to 40 g C $cm^{-2}yr^{-1}$ (Fig. 2), while in southern China, lacustrine CAR varied from 0.6 to 30 g C cm^{-2} yr^{-1} (Fig. 2). The highest CAR reached 200 g C cm^{-2} yr^{-1}, while the lowest was only 0.05 g C cm^{-2} yr^{-1} in both northern and southern lakes. The average CAR values for lakes in northern and southern China were 8.01 and 10.12 g C cm^{-2} yr^{-1}, respectively. The combined CAR Z-score of the northern lakes appeared as a convex shape with high values during 9–3 cal ka BP (Fig. 3e and 5d). In comparison, the combined CAR Z-score of the southern lakes showed a concave shape, with low values during 8–3 cal ka BP (Fig. 3f and 5i).

3.3. Characteristics of precipitation, vegetation, and human activities

Based on synthesized paleosol occurrence results and pollen records, it was found that the maximum precipitation during the Holocene in northern China occurred from 8 to 3 cal ka BP. This is supported by the regionally synthesized record based on pollen, which showed that the annual mean precipitation in northern China reached maximum values from 7.8 to 3.4 cal ka BP (Fig. 4a and b). In contrast, sediment analysis, such as the ratio of Rb/Sr in Nanyihu Lake sediments (Fig. 4f), the IRM record from Heshang Cave (Fig. 4e), the CPI values of n-alkanes in Dahu Lake sediments (Fig. 4d), and the Hopanoid record from Dajiuhu peatland (Fig. 4c), indicate that the mid-Holocene was the driest period during the Holocene. With regard to vegetation changes, the ratio of AP/NAP in northern China exhibited an initial increase followed by a decrease, while in southern China, the ratio of AP/NAP showed a downward trend since the beginning of the Holocene (Fig. 5e and j). Indicators reflecting the intensity of human activities, such as the density average estimates for archaeological sites in both northern and southern China (Fig. 6a and c), as well as the historical cropland area estimates in China (Fig. 6d), show an increasing trend since 6 cal ka BP. Additionally, in the lower Yangtze River region, the proportion of domesticated rice spikelet bases and double-peaked phytoliths significantly increased after 6 cal ka BP (Fig. 6b).

3.4. Contrasting pattern in lacustrine CAR in north-south China

From 12 to 6 cal ka BP, CAR in northern China increased in line with a rise in monsoon precipitation (Fig. 5c and d). Conversely, CAR decreased during the same period in southern China, corresponding to a decrease in monsoon precipitation (Fig. 5h and i). Since 6 cal ka BP, CAR has exhibited a decreasing trend in northern China, which aligns with a

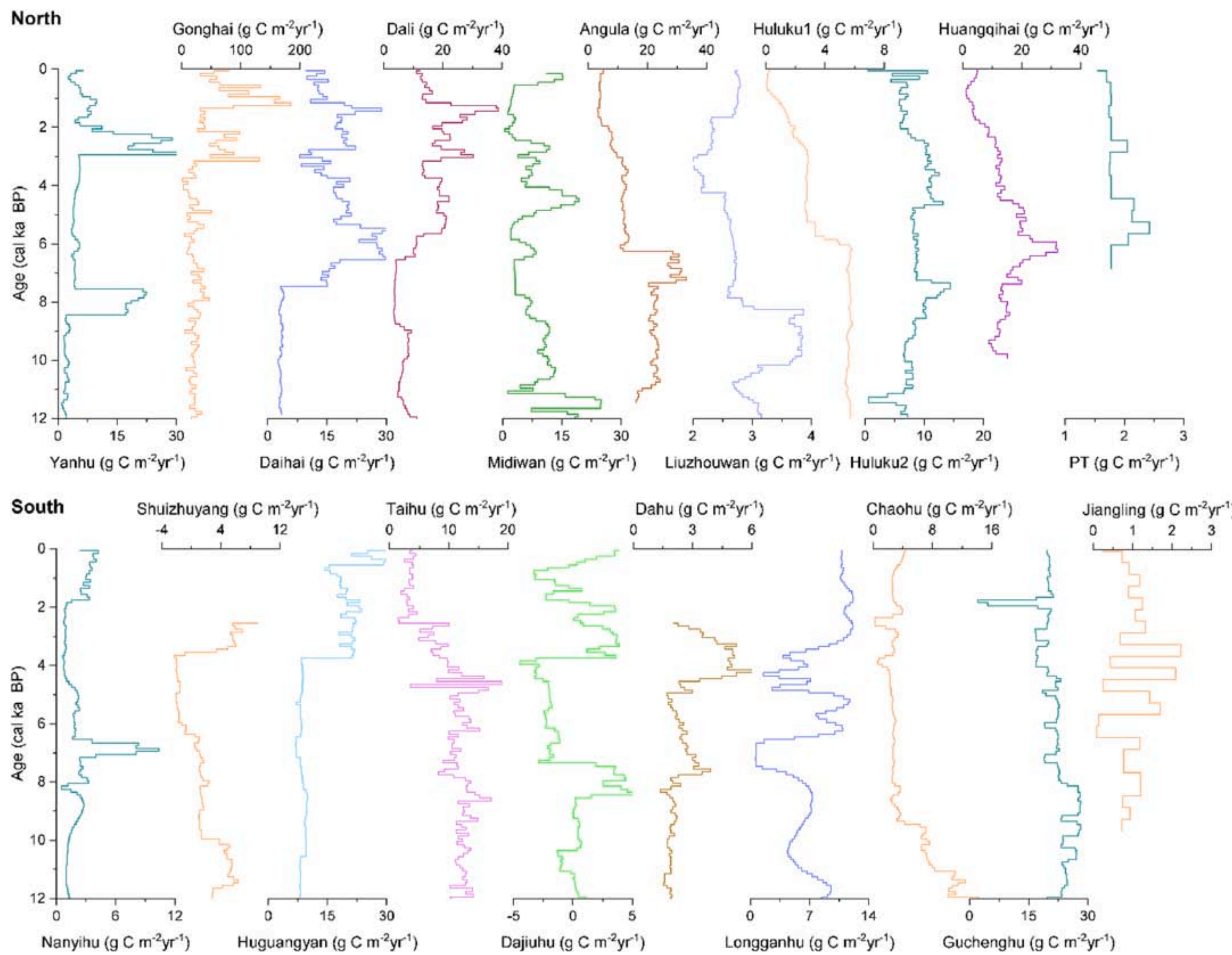

Fig. 2. Variations of carbon accumulation rate (CAR, g C m^{-2} yr^{-1}) in the lakes from northern and southern China during the Holocene.

reduction in precipitation and an increase in human activities (Fig. 5c and d, 6). In contrast, there has been an increase in precipitation and human activities in southern China, which corresponds to a rise in CAR (Fig. 5h and i, 6). The changes in lacustrine CAR were positively correlated with moisture levels in both northern (with statistical significance at $^{*}P < 0.1$, explaining 27.7% of the variance; see Fig. 7a) and southern China (with statistical significance at $^{**}P < 0.01$, explaining 26.2% of the variance; see Fig. 7b).

4. Discussion

4.1. Monsoon precipitation dominated lacustrine C accumulation during the period 11–6 cal ka BP

Water availability plays a crucial role in the distribution of natural vegetation on Earth's land surface. Soil moisture is crucial for photosynthesis and the survival of terrestrial plants (Gerten et al., 2004; Zhang et al., 2020). Analysis of data from northern and southern China shows that the change in monsoon precipitation from 11 to 6 cal ka BP follows a trend similar to the curve of the ratio of arboreal to non-arboreal pollen (AP/NAP) (Fig. 5). This suggests that increased precipitation leads to a higher proportion of arboreal plants.

In lake systems, the input of terrigenous debris and organic soil significantly contributes to the accumulation of organic C in the sediments. Vascular plants, such as shrubs and trees, which have woody and cellulosic tissues, are better preserved in lake sediments compared to nonvascular plants. From 11 to 6 cal ka BP, the proportion of arboreal pollen in northern China increased (Fig. 5e), indicating the expansion of trees during that peiod. Trees growing in lake basins produce more decomposition-resistant C, resulting in higher TOC accumulation in lake sediments. While both TOC and the ratio of AP/NAP showed downward trends from 11 to 6 cal ka BP, the TOC trend is consistent with the ratio of AP/NAP in both northern and southern China (Fig. 5). This suggest that the expansion of trees had a major influence on the observed changes in carbon accumulation in lake sediments. Our data integration study has indicated that there is a positive correlation between the proportion of arboreal vegetation and TOC in sediments, although aquatic species can also affect the accumulation of carbon in lake systems.

The sediments accumulated in lakes can provide information about historical rates of sedimentation and soil erosion (Wren and Davidson, 2011). For many lakes, SR in central, deep water cores can typically provide a good approximation of gross changes in the rate of allochthonous inputs related to soil erosion (Dearing, 1991). There is well-known dependence between precipitation and mean annual sediment yields (Langbein and Schumm, 1958) as increased precipitation favours soil erosion. However, higher precipitation also promoted the growth of arboreal plants, which might have caused a decline in the rate of soil erosion by increasing vegetation cover. Thus, precipitation's direct and indirect effects have opposite results on lake SR. When

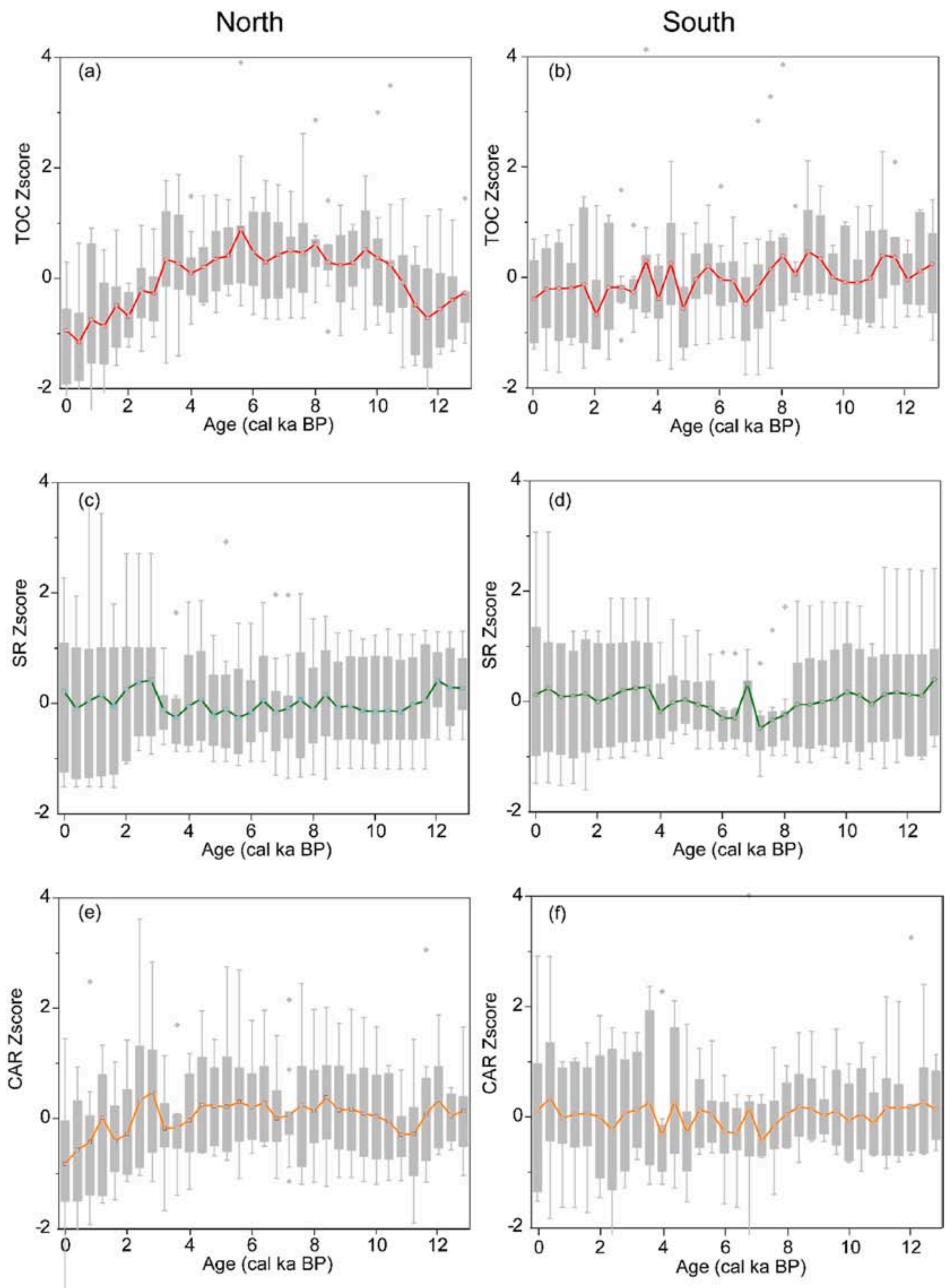

Fig. 3. Temporal patterns of total carbon content (TOC), sediment rate (SR), and carbon accumulation rate (CAR) at 400-year bins for lake sediment records in northern (a, c, e) and southern China (b, d, f). The box plot for each bin shows the mean value (open circles connected by red-color curve), the interquartile range of data (bar); the maximum and minimum values (whiskers); and the outliers (diamonds).

analyzing the SR of lakes in northern and southern China, we found that it closely follows the trends in precipitation (Fig. 5). This suggests that the increase or decrease in arboreal plants in the catchment did not significantly affect the SR and the input rate of terrestrial plant debris. This may be because the enhanced precipitation only raised the content of the arboreal plants but did not necessarily increase the vegetation coverage, which did not indirectly decrease soil erosion, and vice versa. Therefore, the direct impact of precipitation on soil erosion is stronger than the indirect impact through vegetation cover in northern and southern China.

When soil erosion occurs in the catchment, dead and fallen vegetation is transported into the lakes. Increased soil erosion due to higher precipitation results in faster sediment accumulation and input of terrestrial plant debris into lakes. This process not only enhances the TOC in lake sediments but also increases the SR of lakes. Studies conducted in northern China show that between 11 and 6 cal ka BP the CAR

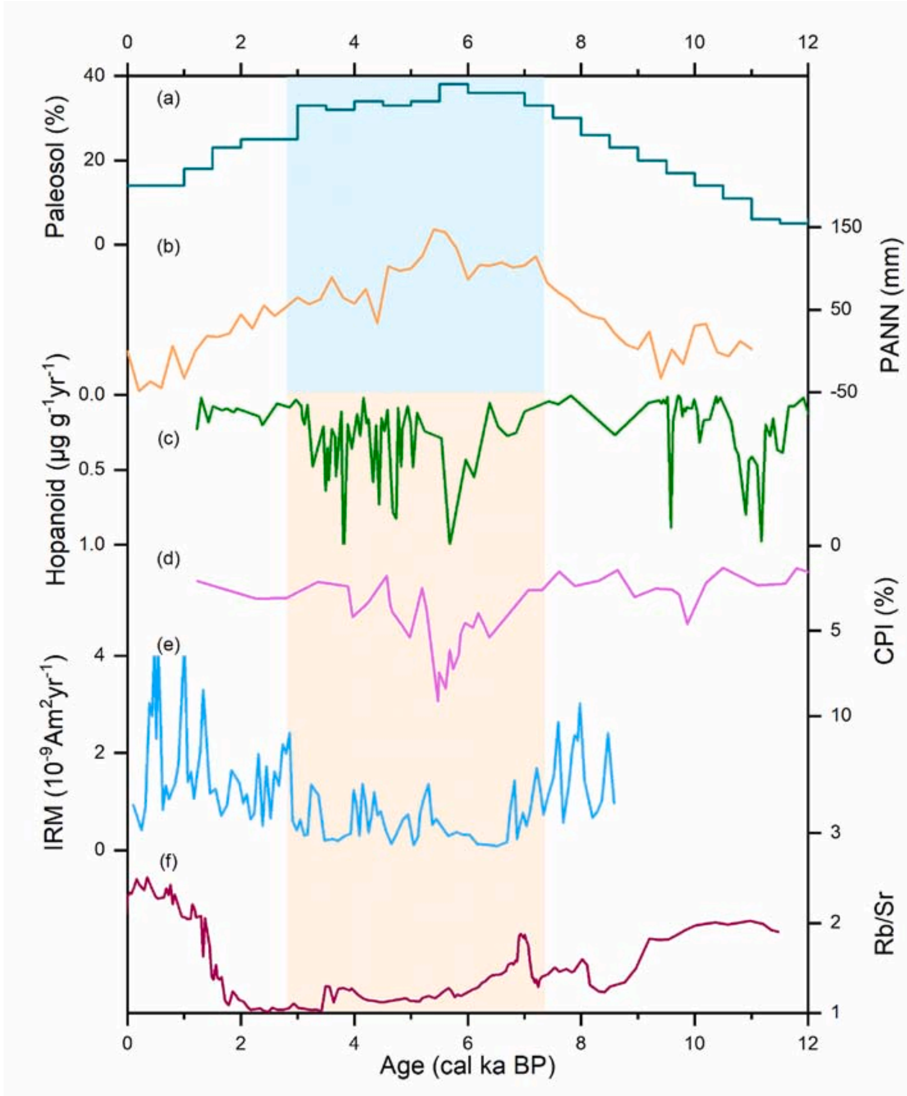

Fig. 4. Holocene paleo-moisture records from northern and southern China. (a) Percentage change in paleosol of the East Sandy Land in northern China (Li et al., 2014); (b) A compiled anomaly record for Holocene annual mean precipitation (PANN) reconstructed from pollen records in northern China (Li et al., 2018); (c) Hopanoid flux of the Dajiuhu peatland (Xie et al., 2013); (d) Carbon preference index (CPI) of n-alkanes in the Dahu Lake (Zhou et al., 2005); (e) Environmental magnetic record of speleothems from Heshang Cave (Zhu et al., 2017); (f) Rb/Sr ratio of Nayihu Lake (Liu et al., 2020).

increased. This increase can be attributed to the amplified monsoon precipitation, which promoted the increase in TOC and SR in lake sediments. In contrast, southern China experienced a decrease in CAR during the same period due to weakened monsoon precipitation. This decrease occurred because there was reduced TOC and SR in lake sediments in the region. The analysis of TOC and the AP/NAP pollen ratio data emphasized that increased monsoon precipitation promotes higher TOC content and SR in lake sediments, while reduced monsoon precipitation leads to lower TOC content and SR in lake sediments. Specifically, the observed changes in CAR were found to be positively correlated with moisture levels in both northern and southern China, as determined by using a GAM regression model (Fig. 7).

4.2. Both precipitation and human activities affect lacustrine C accumulation since 6 cal ka BP

The concentration of Neolithic sites, the presence of domesticated rice, and the expansion of cropland in China all indicate that the rapid development of human activities since 6 cal ka BP (Fig. 6). This development coincided with the mixing of the human population in both northern and southern China during the Neolithic period (Yang et al., 2020). Around 5–6 cal ka BP, human activities, such as deforestation and land cultivation, likely caused permanent changes to the natural vegetation trend (Cheng et al., 2018). These activities led to a decrease in the number of arboreal plants, resulting in a reduction of carbon input from refractory sources to the lakes. In northern China, both decreased monsoon precipitation and increased human activities contributed to the decline in TOC in lake sediments since 6 cal ka BP (Fig. 5a). In contrast, despite increased monsoon precipitation in southern China, the proportion of arboreal pollen remained low and stable from 6 to 0 cal ka BP, possibly due to intensified agricultural practices. The practices resulted in a sifnificant decrease in tree pollen and a rapid increase in ferns and herbs in the lake sediments in southern China (Zhou et al., 2004). Precipitation can promote an increase in TOC, but human activities have the opposite effect. As a result, the TOC of lake sediments remained stable from 6 to 0 cal ka BP, despite high monsoon precipitation during that period (Fig. 5f).

In northern China, due to the weakening of monsoon precipitation and the increase in human activities, there was no noticeable trend in the SR of lakes after 6 cal ka BP (Fig. 5b, d, 6). Human activities such as

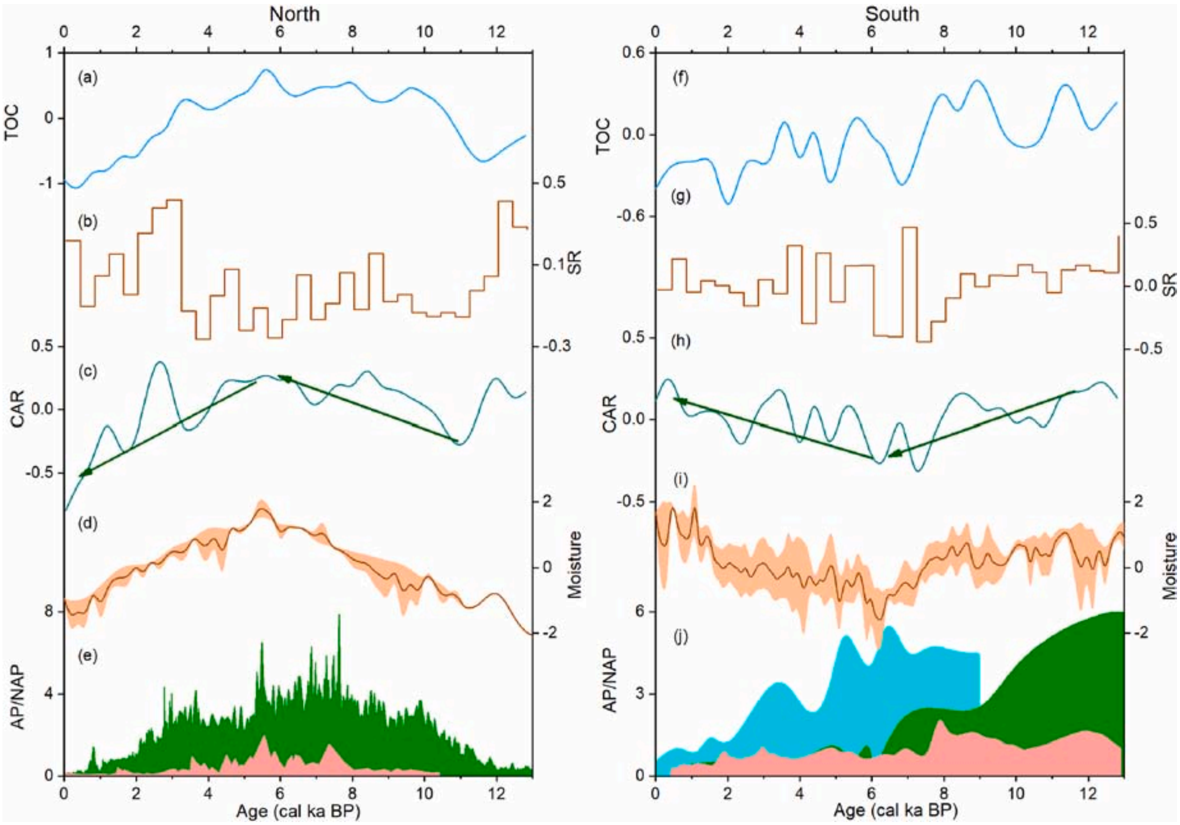

Fig. 5. Comparison of carbon accumulation and its driving factors in lakes of northern and southern China. (a) The combined total carbon content (TOC) Zscore of northern lakes; (b) The combined sediment accumulation rate (SR) Zscore of northern lakes; (c) The combined carbon accumulation rate (CAR) Zscore of northern lakes; (d) The composite moisture Zscore of northern China; (e) The AP/NAP pollen ratio of northern China, the pollen record from Gonghai Lake (green shadow) (Chen et al., 2015a) and Daihai Lake (pink shadow) (Xu et al., 2010); (f) The combined TOC Zscore of southern lakes; (g) The combined SR Zscore of southern lakes; (h) The combined CAR Zscore of southern lakes; (i) The composite moisture Zscore of southern China; (j) The AP/NAP pollen ratio of southern China, the pollen record from Nanyihu Lake (cyan shadow) (Chen et al., 2021), Dahu Lake (green shadow) (Zhou et al., 2004) and Huguangyan Lake (pink shadow) (Wang et al., 2007).

agriculture, grazing, and logging can promote the SR of lake sediments. However, under the conditions of decreasing precipitation and reduced runoff, soil erosion becomes less likely to occur. The precipitation gradually weakened and human activities gradually increased in northern China after 6 cal ka BP. The decrease in precipitation led to a lower SR, while increased human activities resulted in a higher SR. These opposing influences resulted in no clear trend in the SR. Additionally, weakened rainfall does not necessarily indirectly increase soil erosion or the input rates of terrestrial plant debris by reducing arboreal vegetation. In southern China, the SR of lake sediments exhibited an upward trend from 6 to 0 cal ka BP (Fig. 5g) due to the positive relationship between enhanced human activities, increased precipitation, and SR. The effects of civilization and intensive agriculture in southern China caused significantly higher erosion rates compared to undisturbed land (Nearing et al., 2017). Increased precipitation provided the driving force for soil erosion and may have promoted the growth of arboreal plants. However, the low ratio of AP/NAP during 6–0 cal ka BP suggests that precipitation's indirect impact on vegetation coverage was limited. Therefore, The combination of increased precipitation and human activities greatly contributed to the rise in SR in southern China since 6 cal ka BP.

Regarding the changing concentration of CAR, it exhibited a decreasing trend from 6 to 0 cal ka BP in northern China due to the combined effects of weakened precipitation and enhanced human activities, which reduced the TOC content in lake sediments. The SR of lakes followed no apparent trend, so TOC dominated the trend of CAR in northern China after 6 cal ka BP. In contrast, in southern China during 6–0 cal ka BP, increased precipitation and human activities led to an increase in land soil runoff, resulting in a rise in CAR. The TOC in lake sediments did not show any significant trend. Therefore, the CAR in southern China was mainly dominated by SR.

4.3. North-south difference of lacustrine C accumulation in China during the Holocene

An increasingly accepted point of view is that the highest levels of EASM rainfall occurred during the mid-Holocene (Liu et al., 2020). However, there is still controversy regarding precipitation patterns in southern China during the Holocene. Nonetheless, multiple high-quality paleo-precipitation reconstructions indicate that monsoon rainfall was low in southern China during the mid-Holocene and high during the early and late Holocene. Various indicators such as sediment Rb/Sr ratios in Nanyihu Lake, the IRM record from Heshang Cave, the Hopanoid record from Dajiuhu peatland, and the CPI values of n-alkanes in Dahu Lake sediments all support the idea that the mid-Holocene was the driest period of the Holocene (Fig. 4). This suggests a dipole pattern of monsoon precipitation between northern and southern China, with the movement of the WPSH causing an anti-phase in rainfall between the two regions. When the WPSH retreats northeastward, the rainfall belt migrates northward, resulting in reduced precipitation in southern China and increased precipitation in northern China, and vice versa (Liu et al., 2020).

Between 11 and 6 cal ka BP, monsoon precipitation exhibited an increasing trend in northern China. The increased precipitation had two effects: firstly, it promoted the growth of trees, leading to an increase in TOC content in lake sediments; secondly, it increased runoff, leading to

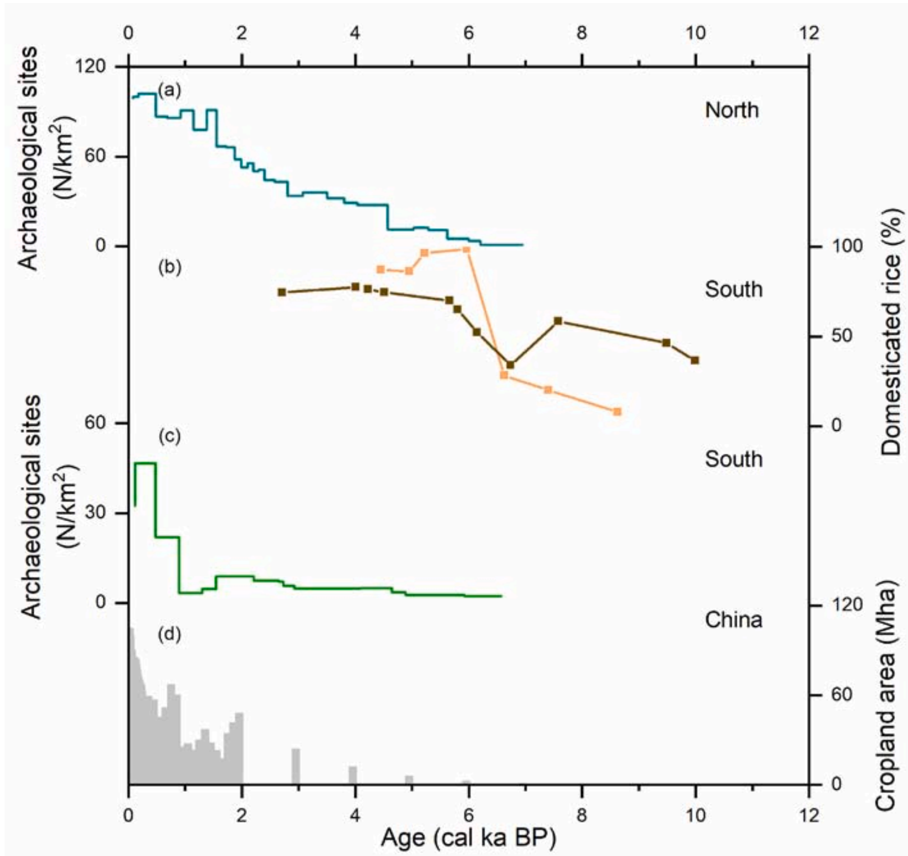

Fig. 6. The intensity of human activities in China during the Holocene. (a) Density estimates of archaeological sites (number of sites per km^{-2}) in northern China (Hosner et al., 2016); (b) the proportion of domesticated rice spikelet bases (orange line) and double-peaked phytoliths (brown line) (Ma et al., 2018); (c) density estimates of archaeological sites in southern China (Hosner et al., 2016); (d) historical cropland area estimates in China (Goldewijk et al., 2017).

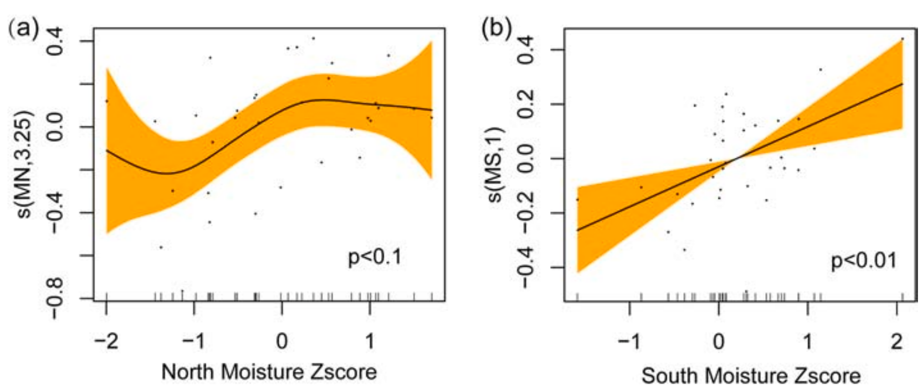

Fig. 7. Fitted smooth function between lacustrine carbon accumulation rate (CAR) and moisture from a general additive model (GAM) for lake sites in northern and southern China. The orange shadings mark the 95% uncertainty interval of the fitted function. The dots show the distribution of observed values for the CAR and moisture values. The number in parenthesis is the effective degrees of freedom (edf) of the smooth function.

soil erosion and an accelerated SR in lakes (Fig. 8a). Consequently, enhanced precipitation not only increased TOC levels but also resulted in higher SR, leading to a higher concentration of CAR in lakes in northern China during 11–6 cal ka BP. In contrast, during the time period from 11 to 6 cal ka BP, there was a noticeable decline in monsoon precipitation in southern China. This decrease in rainfall had significant consequences on the local environment. One of the impacts was reflected in the species composition of the vegetation found in the region. As precipitation decreased, there was a lower proportion of trees and shrubs, in the region (Fig. 5j). Therefore, the decline in precipitation also had an effect on the levels of TOC in the sediments of lakes in southern China. With less rainfall, there was a reduced input of organic matter from terrestrial sources into the lakes. As a consequence, the TOC levels in lake sediments decreased during this period (Fig. 5f). Furthermore, the reduced rainfall had an impact on the hydrological processes within the lakes. With lower precipitation, there was a decrease in the amount of runoff and sediment deposition in the lakes (Fig. 5g). As a result, weakened precipitation led to decreased TOC and SR of lakes in southern China, resulting in a decrease in CAR during the period 11–6 cal ka BP (Fig. 8c).

After 6 cal ka BP, human activities gradually increased in both northern and southern China. Additionally, during this period, there was

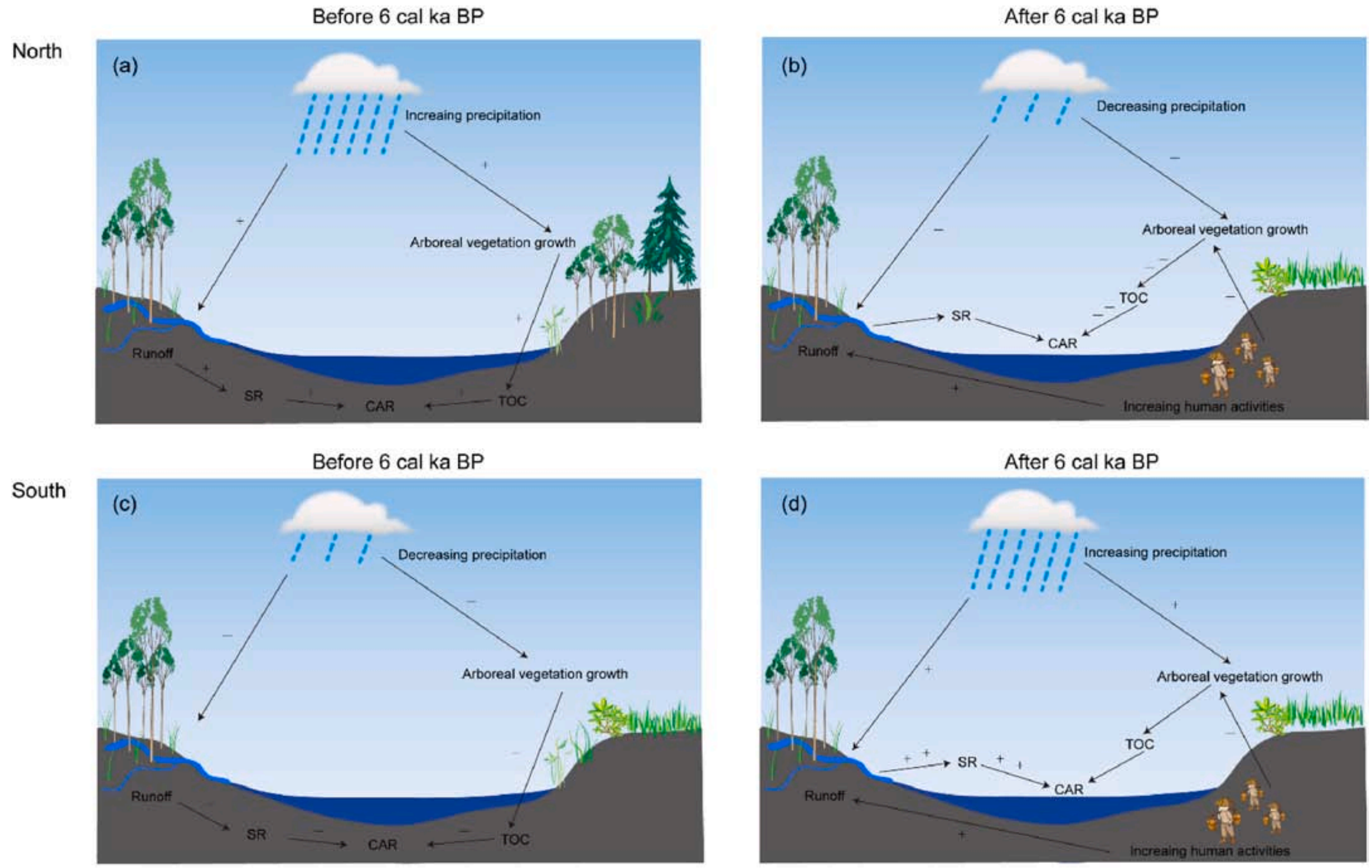

Fig. 8. The conceptual model of lake CAR influenced by monsoon precipitation and human activities during the Holocene. (+) indicates a positive effect, and (−) shows a negative impact. SR is the sediment rate; CAR is the carbon accumulation rate; TOC is the total organic carbon.

a decreasing trend in monsoon precipitation in northern China. The decrease in precipitation had a negative relationship with runoff, while the increasing human activities had a positive relationship with runoff. As a result, the SR in lakes did not show a significant changing trend. However, the decrease in precipitation and the increase in human activities had negative relationships with the growth of arboreal vegetation, leading to a decrease in the TOC content in lake sediments (Fig. 8b). Consequently, the decreasing TOC and stable SR resulted in a decline in CAR in northern China since 6 cal ka BP. On the other hand, southern China experienced an increase in monsoon precipitation during this period. Both the increasing precipitation and human activities contributed to increased runoff and higher SR in lakes. Regarding the TOC content in lake sediments, the increased precipitation promoted the growth of arboreal vegetation, while the intensified human activities reduced the proportion of arboreal vegetation, resulting in no apparent change in the TOC of lake sediments (Fig. 8d). Therefore, the stable TOC and increasing SR caused an increase in CAR in southern China since 6 cal ka BP.

Overall, monsoon precipitation had a positive impact on SR and TOC in lake sediments in both northern and southern China during the Holocene, as determined by using a GAM regression model (Fig. 7). Human activities showed a positive correlation with SR but a negative correlation with TOC. The combined effect of precipitation and human activities led to a decrease in CAR in northern China primarily due to the decrease in TOC, while it resulted in an increase in CAR in southern China mainly due to the increase in SR. Overall, these two factors were more influencial on C accumulation than their opposing effects.

5. Conclusions and implications

(1) There was an inverse phase of C accumulation in lakes between northern and southern China over the Holocene due to the monsoon precipitation differences and human activities.
(2) Monsoon precipitation had a positive correlation with arboreal vegetation and SR in northern and southern China. However, deforestation and farmland reclamation also played an essential role in increased SR and loss of trees since 6 cal ka BP. The indirect impact of precipitation on SR through vegetation coverage was not significant in either northern or southern China during the Holocene.
(3) From 11 to 6 cal ka BP, CAR exhibited an upward trend in northern China due to increased monsoon precipitation, which promoted the accumulation of TOC and SR in lake sediments. In contrast, CAR decreased during the same period in southern China due to weakened monsoon precipitation, resulting in a decline in TOC and SR of lake sediments.
(4) Since 6 cal ka BP, CAR has shown a decreasing trend in northern China, primarily because of reduced precipitation and intensified human activities, which led to a decrease in the TOC content in lake sediments. In contrast, increased precipitation and human activities in southern China have contributed to higher soil erosion and SR in lakes, leading to an increase in CAR.
(5) Our findings address the inconsistencies in the studies of lacustrine C accumulation in the monsoon region of eastern China. By distinguishing between northern and southern lakes, we have clarified the characteristics and influencing factors of lacustrine C accumulation in eastern China during the Holocene. The accumulation of carbon in lake sediments may also be affected by

aquatic species, although comprehensive studies indicate a positive correlation between the proportion of arboreal vegetation and TOC in sediments. Recognizing the north-south difference in CAR and its relationship with monsoon precipitation and human activities can aid in projecting future changes in lake CAR for both regions and understanding their role in the global C cycle.

CRediT authorship contribution statement

Hanxiang Liu: Conceptualization, Methodology, Software, Validation, Formal analysis, Investigation, Resources, Data curation, Writing - original draft, Writing-reviewing and editing, Visualization. **Mengdi Jiang:** Validation, Formal analysis, Writing-reviewing and editing, Supervision. **Zicheng Yu:** Formal analysis, Writing-reviewing and editing. **Wengang Kang:** Writing-reviewing and editing. **Zhongwei Shen:** Resources, Data curation. **Haoran Dong:** Resources. **Shengqian Chen:** Conceptualization, Resources. **Xinwei Yan:** Conceptualization, Writing-reviewing and editing. **Jianbao Liu:** Conceptualization, Validation, Formal analysis, Writing-reviewing and editing, Visualization, Supervision, Project administration, Funding acquisition.

Declaration of competing interest

The authors declare that they have no known competing financial interests or personal relationships that could have appeared to influence the work reported in this paper.

Data availability

Data will be made available on request.

Acknowledgments

This work is supported by the National Science Found for Distinguished Young Scholars (42225105), National Natural Science Foundation of China (42001081), and the Open Fund Project of Key Laboratory of Watershed Surface Processes and Ecological Security, Zhejiang Normal University (KF-2022-13).

Appendix A. Supplementary data

Supplementary data to this article can be found online at https://doi.org/10.1016/j.quascirev.2023.108465.

References

Anderson, N.J., Heathcote, A.J., Engstrom, D.R., 2020. Anthropogenic alteration of nutrient supply increases the global freshwater carbon sink. Sci. Adv. 6, eaaw2145.
Armstrong, A., 2010. Lake carbon. Nat. Geosci. 3, 151-151.
Chen, F., Xu, Q., Chen, J., Birks, H.J.B., Liu, J., Zhang, S., Jin, L., An, C., Telford, R.J., Cao, X., 2015a. East Asian summer monsoon precipitation variability since the last deglaciation. Sci. Rep. 5, 11186.
Chen, J., Chen, F., Feng, S., Huang, W., Liu, J., Zhou, A., 2015b. Hydroclimatic changes in China and surroundings during the medieval climate anomaly and little ice age: spatial patterns and possible mechanisms. Quat. Sci. Rev. 107, 98–111.
Chen, M., Zeng, G., Zhang, J., Xu, P., Chen, A., Lu, L., 2015c. Global landscape of total organic carbon, nitrogen and phosphorus in lake water. Sci. Rep. 5, 15043.
Chen, W., Song, B., Shu, J.-W., Jin, C.-F., Wang, W.-M., 2021. Vegetation history with implication of climate changes and human impacts over the last 9000 years in the Lake Nanyi area, Anhui Province, East China. Palaeoworld 30, 583–592.
Cheng, Z., Weng, C., Steinke, S., Mohtadi, M., 2018. Anthropogenic modification of vegetated landscapes in southern China from 6,000 years ago. Nat. Geosci. 11, 939–943.
Cohen, D.J., 2011. The Beginnings of agriculture in China: a multiregional view. Curr. Anthropol. 52, S273–S293.
Dearing, J.A., 1991. Lake sediment records of erosional processes. Hydrobiologia 214, 99–106.
Ding, Y., 2004. Deposit Record of Climatic and Enviornmental Changes of Taihu Lake Since10,000 a. East China Normal University, Shanghai (Thesis, In Chinese with English abstract).
Ding, Y., Wang, Z., Sun, Y., 2008. Inter-decadal variation of the summer precipitation in East China and its association with decreasing Asian summer monsoon. Part I: observed evidences. Int. J. Climatol. 28, 1139–1161.
Dong, X., Anderson, N.J., Yang, X., chen, X., Shen, J., 2012. Carbon burial by shallow lakes on the Yangtze floodplain and its relevance to regional carbon sequestration. Global Change Biol. 18, 2205–2217.
Dong, H., Chen, Z., Wang, Y., Chen, J., Zhang, Z., Shen, Z., Yan, X., Liu, J., 2024. Impact of water level change on shifts in subsistence regimes revealed by anthropogenic fire in the lower Yangtze basin during the Mid-Holocene. Palaeogeogr. Palaeoclimatol. Palaeoecol. 633, 111902.
Ge, Q., Hao, Z., Zheng, J., Shao, X., 2013. Temperature changes over the past 2000 yr in China and comparison with the Northern Hemisphere. Clim. Past 9, 1153–1160.
Gerten, D., Schaphoff, S., Haberlandt, U., Lucht, W., Sitch, S., 2004. Terrestrial vegetation and water balance—hydrological evaluation of a dynamic global vegetation model. J. Hydrol. 286, 249–270.
Goldewijk, K.K., Beusen, A., Doelman, J., Stehfest, E., 2017. Anthropogenic land use estimates for the Holocene – HYDE 3.2. Earth Syst. Sci. Data 9, 927–953.
Gudasz, C., Bastviken, D., Steger, K., Premke, K., Sobek, S., Tranvik, L.J., 2010. Temperature-controlled organic carbon mineralization in lake sediments. Nature 466, 478–481.
Hao, Q., Liu, H., Yin, Y., Wang, H., Feng, M., 2014. Varied responses of forest at its distribution margin to Holocene monsoon development in northern China. Palaeogeogr. Palaeoclimatol. Palaeoecol. 409, 239–248.
Hao, Q., Yang, S., Song, Z., Wang, Z., Yu, C., Wang, H., 2021. Vegetation determines lake sediment carbon accumulation during Holocene in the forest–steppe ecotone in northern China. Forests 12, 696.
Hastie, T., Tibshirani, R., 1986. Generalized additive models. Stat. Sci. 1, 297–318.
Hosner, D., Wagner, M., Tarasov, P.E., Chen, X., Leipe, C., 2016. Spatiotemporal distribution patterns of archaeological sites in China during the Neolithic and Bronze Age: an overview. Holocene 26, 1576–1593.
Hu, F., Yang, Y., Zhang, J., Zheng, H., 2015. Sedimentary environmental evolution during last deglaciation and early Holocene in Chaohu region. Mar. Geol. Quat. Geol. 35, 153–162 (In Chinese with English abstract).
Kastowski, M., Hinderer, M., Vecsei, A., 2011. Long-term carbon burial in European lakes: analysis and estimate. Global Biogeochem. Cycles 25, GB3019.
Kaufman, D., McKay, N., Routson, C., Erb, M., Davis, B., Heiri, O., Jaccard, S., Tierney, J., Dätwyler, C., Axford, Y., Brussel, T., Cartapanis, O., Chase, B., Dawson, A., de Vernal, A., Engels, S., Jonkers, L., Marsicek, J., Moffa-Sánchez, P., Morrill, C., Orsi, A., Rehfeld, K., Saunders, K., Sommer, P.S., Thomas, E., Tonello, M., Tóth, M., Vachula, R., Andreev, A., Bertrand, S., Biskaborn, B., Bringué, M., Brooks, S., Caniupán, M., Chevalier, M., Cwynar, L., Emile-Geay, J., Fegyveresi, J., Feurdean, A., Finsinger, W., Fortin, M.-C., Foster, L., Fox, M., Gajewski, K., Grosjean, M., Hausmann, S., Heinrichs, M., Holmes, N., Ilyashuk, B., Ilyashuk, E., Juggins, S., Khider, D., Koinig, K., Langdon, P., Larocque-Tobler, I., Li, J., Lotter, A., Luoto, T., Mackay, A., Magyari, E., Malevich, S., Mark, B., Massaferro, J., Montade, V., Nazarova, L., Novenko, E., Pařil, P., Pearson, E., Peros, M., Pienitz, R., Płóciennik, M., Porinchu, D., Potito, A., Rees, A., Reinemann, S., Roberts, S., Rolland, N., Salonen, S., Self, A., Seppä, H., Shala, S., St-Jacques, J.-M., Stenni, B., Syrykh, L., Tarrats, P., Taylor, K., van den Bos, V., Velle, G., Wahl, E., Walker, I., Wilmshurst, J., Zhang, E., Zhilich, S., 2020. A global database of Holocene paleotemperature records. Sci. Data 7, 115.
Kortelainen, P., Pajunen, H., Rantakari, M., Saarnisto, M., 2004. A large carbon pool and small sink in boreal Holocene lake sediments. Global Change Biol. 10, 1648–1653.
Langbein, W.B., Schumm, S.A., 1958. Yield of sediment in relation to mean annual precipitation. Eos, Transactions American Geophysical Union 39, 1076–1084.
Li, J., Yan, H., Dodson, J., Xu, Q., Sun, A., Cheng, B., Li, C., Ni, J., Zhang, X., Lu, F., 2018. Regional-scale precipitation anomalies in northern China during the Holocene and possible impact on prehistoric demographic changes. Geophys. Res. Lett. 45 (12), 477-412,486.
Li, Q., Wu, H., Yu, Y., Sun, A., Marković, S.B., Guo, Z., 2014. Reconstructed moisture evolution of the deserts in northern China since the last glacial maximum and its implications for the East Asian summer monsoon. Global Planet. Change 121, 101–112.
Li, Y., 2019. The Climate Change since the Last Glacial Maximum Recorded by the Sediment Core of Yanhu Lake in Yuncheng, Shanxi Province. China University of Geosciences Wuhan (Thesis, In Chinese with English abstract).
Liu, J., Shen, Z., Chen, W., Chen, J., Zhang, X., Chen, J., Chen, F., 2020. Dipolar mode of precipitation changes between north China and the Yangtze River Valley existed over the entire Holocene: evidence from the sediment record of Nanyi Lake. Int. J. Climatol. 41, 1667–1681.
Liu, J., Wang, Y., Wang, Y., Guan, Y., Dong, J., Li, T., 2018. A multi-proxy record of environmental changes during the Holocene from the Haolaihure Paleolake sediments, Inner Mongolia. Quat. Int. 479, 148–159.
Liu, Z., Zhu, J., Rosenthal, Y., Zhang, X., Ottobliesner, B.L., Timmermann, A., Smith, R.S., Lohmann, G., Zheng, W., Timm, O., 2014. The Holocene temperature conundrum. Proc. Natl. Acad. Sci. USA 111, 201407229.
Ma, Y., Yang, X., Huan, X., Gao, Y., Wang, W., Li, Z., Ma, Z., Perry, L., Sun, G., Jiang, L., Jin, G., Lu, H., 2018. Multiple indicators of rice remains and the process of rice domestication: a case study in the lower Yangtze River region, China. PLoS One 13, e0208104.
Nearing, M.A., Xie, Y., Liu, B., Ye, Y., 2017. Natural and anthropogenic rates of soil erosion. International Soil and Water Conservation Research 5, 77–84.
Wang, H., Liu, H., Cui, H., Abrahamsen, N., 2001. Terminal Pleistocene/Holocene palaeoenvironmental changes revealed by mineral-magnetism measurements of lake sediments for Dali Nor area, southeastern Inner Mongolia Plateau, China. Palaeogeogr. Palaeoclimatol. Palaeoecol. 170, 115–132.

Wang, H., Liu, H., Zhu, J., Yin, Y., 2010. Holocene environmental changes as recorded by mineral magnetism of sediments from Anguli-nuur Lake, southeastern Inner Mongolia Plateau, China. Palaeogeogr. Palaeoclimatol. Palaeoecol. 285, 30–49.

Wang, L., Hu, S., Yu, G., Wang, X., Wang, Q., Zhang, Z., Ma, M., Cui, B., Liu, X., 2019. Multiproxy studies of lake sediments during mid-Holocene in Zhengzhou region of the Henan Province, central China, and the implications for reconstructing the paleoenvironments. Quat. Int. 521, 104–110.

Wang, M., Chen, H., Yu, Z., Wu, J., Zhu, Q.a., Peng, C., Wang, Y., Qin, B., 2015. Carbon accumulation and sequestration of lakes in China during the Holocene. Global Change Biol. 21, 4436–4448.

Wang, Q., Li, C., Xie, Y., 2006. Sedimentary records of paleoclimate evolution in the Jiangling area of the Jianghan Plain since 9ka. J. Lake Sci. 18, 280–284 (In Chinese with English abstract).

Wang, S., Lü, H., Liu, J., Negendank, J.F.W., 2007. The early Holocene optimum inferred from a high-resolution pollen record of Huguangyan Maar Lake in southern China. Chin. Sci. Bull. 52, 2829–2836.

Wang, S., Yang, X., Ma, Y., Pan, H., Tong, G., Wu, X., 1996. Relationship between environmental changes and palaeo-monsoon in gucheng lake, Jiangsu province since 15 ka. Sci. China E 26, 137–141 (In Chinese with English abstract).

Wren, D., Davidson, G., 2011. Using lake sedimentation rates to quantify the effectiveness of erosion control in watersheds. J. Soil Water Conserv. 66, 313–322.

Xiao, J., Si, B., Zhai, D., Itoh, S., Lomtatidze, Z., 2008. Hydrology of dali lake in central-eastern inner Mongolia and Holocene East Asian monsoon variability. J. Paleolimnol. 40, 519–528.

Xiao, J., Wu, J., Si, B., Liang, W., Nakamura, T., Liu, B., Inouchi, Y., 2006. Holocene climate changes in the monsoon/arid transition reflected by carbon concentration in Daihai Lake of Inner Mongolia. Holocene 16, 551–560.

Xie, S., Evershed, R.P., Huang, X., Zhu, Z., Pancost, R.D., Meyers, P.A., Gong, L., Hu, C., Huang, J., Zhang, S., 2013. Concordant monsoon-driven postglacial hydrological changes in peat and stalagmite records and their impacts on prehistoric cultures in central China. Geology 41, 827–830.

Xu, Q., Xiao, J., Li, Y., Tian, F., Nakagawa, T., 2010. Pollen-based quantitative reconstruction of Holocene climate changes in the Daihai lake area, Inner Mongolia, China. J. Clim. 23, 2856–2868.

Yancheva, G., Nowaczyk, N.R., Mingram, J., Dulski, P., Schettler, G., Negendank, J.F.W., Liu, J., Sigman, D.M., Peterson, L.C., Haug, G.H., 2007. Influence of the intertropical convergence zone on the East Asian monsoon. Nature 445, 74–77.

Yang, M.A., Fan, X., Sun, B., Chen, C., Lang, J., Ko, Y.C., Tsang, C.H., Chiu, H., Wang, T., Bao, Q., Wu, X., Hajdinjak, M., Ko, A.M., Ding, M., Cao, P., Yang, R., Liu, F., Nickel, B., Dai, Q., Feng, X., Zhang, L., Sun, C., Ning, C., Zeng, W., Zhao, Y., Zhang, M., Gao, X., Cui, Y., Reich, D., Stoneking, M., Fu, Q., 2020. Ancient DNA indicates human population shifts and admixture in northern and southern China. Science 369, 282–288.

Yang, X., Yanhong, W.U., Zhu, Y., Wang, S., Shen, J., 2002. Environmental changes revealed by lacustrine sediment from longgan lake since last glacial maximum. J. Lake Sci. 14, 106–109 (In Chinese with English abstract).

Zhang, F., Xue, B., Yao, S., Gui, Z., 2013. The organic carbon burial rates in Chinese lake sediments during Holocene Megatherma. Quat. Sci. 33, 401–402 (In Chinese with English abstract).

Zhang, Y., Parazoo, N.C., Williams, A.P., Zhou, S., Gentine, P., 2020. Large and projected strengthening moisture limitation on end-of-season photosynthesis. Proc. Natl. Acad. Sci. USA 117, 9216–9222.

Zhou, W., Donahue, D.J., Porter, S.C., Jull, A.J.T., Li, X., Stuiver, M., An, Z., Matsumoto, E., Dong, G., 1996. Variability of monsoon climate in East asia at the end of the last glaciation. Quat. Res. 46, 219–229.

Zhou, W., Yu, X., Jull, A.T., Burr, G., Xiao, J., Lu, X., Xian, F., 2004. High-resolution evidence from southern China of an early Holocene optimum and a mid-Holocene dry event during the past 18,000 years. Quat. Res. 62, 39–48.

Zhou, W.J., Xie, S.C., Meyers, P.A., Zheng, Y.H., 2005. Reconstruction of late glacial and Holocene climate evolution in southern China from geolipids and pollen in the Dingnan peat sequence. Org. Geochem. 36, 1272–1284.

Zhu, Z., Feinberg, J.M., Xie, S., Bourne, M.D., Huang, C., Hu, C., Cheng, H., 2017. Holocene ENSO-related cyclic storms recorded by magnetic minerals in speleothems of central China. Proc. Natl. Acad. Sci. U.S.A. 114, 852–857.